Clonal-level lineage commitment pathways of hematopoietic stem cells in vivo

Rong Lu[a,b,1], Agnieszka Czechowicz[a,c,2], Jun Seita[a,3], Du Jiang[b], and Irving L. Weissman[a,c,1]

[a]Institute for Stem Cell Biology and Regenerative Medicine, Stanford University School of Medicine, Stanford, CA 94305; [b]Department of Stem Cell Biology and Regenerative Medicine, Eli and Edythe Broad Center for Regenerative Medicine and Stem Cell Research, Keck School of Medicine, University of Southern California, Los Angeles, CA 90033; and [c]Department of Developmental Biology, Stanford University School of Medicine, Stanford, CA 94305

Contributed by Irving L. Weissman, December 3, 2018 (sent for review January 26, 2018; reviewed by Iannis Aifantis, Craig T. Jordan, and Amy J. Wagers)

While the aggregate differentiation of the hematopoietic stem cell (HSC) population has been extensively studied, little is known about the lineage commitment process of individual HSC clones. Here, we provide lineage commitment maps of HSC clones under homeostasis and after perturbations of the endogenous hematopoietic system. Under homeostasis, all donor-derived HSC clones regenerate blood homogeneously throughout all measured stages and lineages of hematopoiesis. In contrast, after the hematopoietic system has been perturbed by irradiation or by an antagonistic anti-ckit antibody, only a small fraction of donor-derived HSC clones differentiate. Some of these clones dominantly expand and exhibit lineage bias. We identified the cellular origins of clonal dominance and lineage bias and uncovered the lineage commitment pathways that lead HSC clones to different levels of self-renewal and blood production under various transplantation conditions. This study reveals surprising alterations in HSC fate decisions directed by conditioning and identifies the key hematopoiesis stages that may be manipulated to control blood production and balance.

hematopoietic stem cell | clonal tracking | lineage commitment | transplantation preconditioning | radiation

Hematopoietic stem cells (HSCs) sustain the blood and immune systems through a complex lineage commitment process (1–3). This process involves several steps during which HSCs become progressively more specified in their potential and eventually give rise to mature blood and immune cells with distinct functions. This stepwise lineage commitment forms the basis of the hematopoietic hierarchy and establishes a paradigm for studying cellular development, differentiation, and malignancy. While the hematopoietic hierarchy has been extensively studied to describe the aggregate differentiation of the HSC population, little is known about the lineage commitment process of individual HSC clones.

Knowledge of HSC clonal-level lineage commitment can reveal new insights into HSC regulatory mechanisms. Many regulatory factors act on individual HSCs and not on the HSC population as a whole. For example, the microenvironment, or niche, extends throughout the body and regulates HSCs through direct contact and through the tuning of local cytokine concentrations (4–7). The distinct characteristics of HSC clones have also been inferred by several recent studies on the clonality of blood cells, suggesting that HSC clones are heterogeneous and possess differentiation preferences toward either myeloid or lymphoid lineages (8–18). Although such lineage bias is averaged at the population level, it plays important roles in aging, immune deficiency, and many hematopoietic disorders involving an unbalanced hematopoietic system (8, 14, 19–22). The existence of lineage bias indicates that HSC differentiation at the population level is an amalgamation of diverse lineage commitments of individual HSC clones. Disentangling the heterogeneity of hematopoiesis not only is essential for understanding HSC regulatory mechanisms but may also provide new insights into the origin of hematological diseases, identify new therapeutic targets, and illuminate better understanding of HSC transplantation which may ultimately improve HSC-based clinical treatments.

Irradiation-mediated transplantation is used in the vast majority of HSC studies, including those suggesting HSC lineage bias (8, 10, 12, 13, 15). HSCs are usually purified using cell-surface markers ex vivo and then transplanted and studied in a different host, where the activities of donor HSCs can be distinguished from those of other cells (1–3, 23). The transplantation procedure is almost always accompanied by irradiation (1–3, 23), which enhances donor HSC engraftment by massively depleting the recipient's endogenous HSCs and other blood and immune cells (24). It is also widely used in the clinical treatment of cancers and hematopoietic disorders to eliminate diseased cells. Alternative pretransplantation conditioning regimens have recently been developed using anti-ckit antibodies (25, 26). In particular, previous mouse studies have revealed that antagonistic anti-ckit antibody ACK2 can selectively eradicate hematopoietic stem and progenitor cells in certain disease backgrounds while leaving mature hematopoietic cells intact (26, 27). This targeted regimen perturbs the hematopoietic system to a lesser degree than irradiation yet enables robust HSC engraftment.

While preconditioning the recipient is necessary to obtain high levels of HSC engraftment, all conditioning regimens, to various degrees, injure and derange the niches that normally regulate

Significance

Hematopoietic stem cells (HSCs) are the key therapeutic component of bone marrow transplantation, the first and most prevalent clinical stem cell therapy. HSCs sustain daily and lifelong blood and immune production through a complex stepwise lineage commitment process. In this work, we analyzed HSC lineage commitment at the clonal level and identified HSC regulatory mechanisms that are undetectable by conventional population-level studies. We uncovered distinct HSC clonal pathways that lead to differential blood production and imbalances. Furthermore, we showed that regulation of HSCs transplanted into unconditioned hosts is strikingly different from that after irradiation and after an antagonistic antibody treatment, which has important implications for understanding, interpreting, and optimizing HSC transplantation.

Author contributions: R.L., A.C., and I.L.W. designed research; R.L., A.C., and D.J. performed research; R.L., A.C., and J.S. contributed new reagents/analytic tools; R.L. and A.C. analyzed data; and R.L. wrote the paper.

Reviewers: I.A., New York University School of Medicine; C.T.J., University of Colorado; and A.J.W., Harvard University.

The authors declare no conflict of interest.

[1]To whom correspondence may be addressed. Email: ronglu@usc.edu or irv@stanford.edu.

[2]Present address: Department of Pediatrics, Division of Stem Cell Transplantation and Regenerative Medicine, Stanford University School of Medicine, Stanford, CA 94305.

[3]Present address: AI Based Healthcare and Medical Data Analysis Standardization Unit, Medical Sciences Innovation Hub Program, RIKEN, Tokyo 103-0027, Japan.

This article contains supporting information online at www.pnas.org/lookup/suppl/doi:10.1073/pnas.1801480116/-/DCSupplemental.

Published online January 8, 2019.

HSCs (28, 29). Although damaged niches can be restored to some extent after conditioning, it is unclear whether HSC regulation in restored niches still resembles that under normal physiological conditions. For instance, the fraction of HSCs in the cell cycle is significantly higher in irradiated mice than in untreated mice (30). Additionally, recent studies of hair follicle stem cells and intestinal stem cells suggest that tissue repair and homeostasis may be sustained by distinct stem cells and through different mechanisms (31, 32). Hence, comparing individual HSCs and their subsequent lineage commitment with and without irradiation conditioning is crucial for understanding HSC function.

HSCs can be transplanted without the use of conditioning (26, 33), likely by taking advantage of the natural HSC migration in the peripheral blood (34–36). After unconditioned transplantation, donor HSCs injected into the peripheral blood may home and engraft into available niches generated by endogenous migrating HSCs and subsequently participate in normal hematopoiesis for the rest of the organism's lifetime. Unconditioned transplantation minimally perturbs natural hematopoiesis, provides an important experimental model for studying homeostatic hematopoiesis of HSCs, and provides an opportunity for better understanding unconditioned lentiviral HSC-based gene therapy.

Unfortunately, unconditioned transplantation produces low engraftment rates even after repeat transplantations (26, 33). In vivo tracking of the few individual HSCs that engraft after unconditioned transplantation was technically prohibitive until the recent development of an in vivo clonal tracking technology (37–39). This technology uses genetic barcodes drawn from a large semirandom 33-mer DNA barcode library to label and track individual HSCs. Each barcode uniquely corresponds to a distinct HSC with more than 95% confidence, and the lentiviral vectors deliver the barcodes into quiescent HSCs without altering their properties. DNA barcodes are incorporated into the cellular genome and inherited by progeny cells along with regular genomic DNA. The abundance of a genetic barcode in a cell population is proportional to the number of progeny cells that the original barcoded cell produces. Barcodes are recovered by high-throughput sequencing that reads millions of sequences from each sample and provides quantitative results. Compared with clonal tracking using a viral insertion site (40, 41), this technology offers the improved quantification and high sensitivity necessary for tracking the few HSCs that engraft in unconditioned transplantation. Compared with clonal tracking using transposon tagging (16, 17), this technology allows for quantitative analysis of the clonality of HSCs and HSC-derived hematopoietic progenitors, providing precise quantifications of HSC self-renewal and differentiation. Compared with single-cell transplantation (10, 42), this technology offers high-throughput capacity to simultaneously track many HSCs in a single mouse, and thereby reveals the interactions of different HSC clones in the same host.

Using this high-throughput, high-sensitivity quantitative clonal tracking technology (37), we examined clonal-level HSC differentiation throughout multiple stages of lineage commitment in the absence of conditioning and after conditioning with lethal irradiation or ACK2 treatment. These data provide a comprehensive view of HSC activities at the clonal level and reveal the underlying lineage commitment pathways of HSC clones. The discovery of these clonal pathways identifies key stages of HSC differentiation that may serve as potential targets for the treatment of hematopoietic disorders and informs the future improvements of HSC-based therapies.

Results

Purified mouse HSCs [lineage (CD3, CD4, CD8, B220, Gr1, Mac1, Ter119)$^-$/ckit$^+$/Sca1$^+$/Flk2$^-$/CD34$^-$/CD150$^+$] were genetically labeled with unique 33-bp barcodes at the single-cell level using a lentiviral vector before transplantation (Fig. 1*A*). The genetic barcode was inherited by every progeny of a barcoded HSC through cell division and differentiation. Thus, the viral labeling established a one-to-one mapping of a single HSC clone with a unique barcode (37). Donor-derived HSCs and their progeny were harvested 22 wk after transplantation, when blood reconstitution had returned to a steady state (2, 10, 23, 43, 44). To minimize sampling error, peripheral blood cells were obtained through animal perfusion and analyzed in their entirety, and bone marrow cells were obtained and analyzed from the entire crushed contents of all limb bones. Barcodes recovered from these hematopoietic populations were subsequently identified and quantified using high-throughput sequencing.

The number of times that a sequencer detects a unique barcode sequence is referred to as the barcode copy number, indicating the abundance of the barcode in a cell population. This number is proportional to the number of cells that carry the

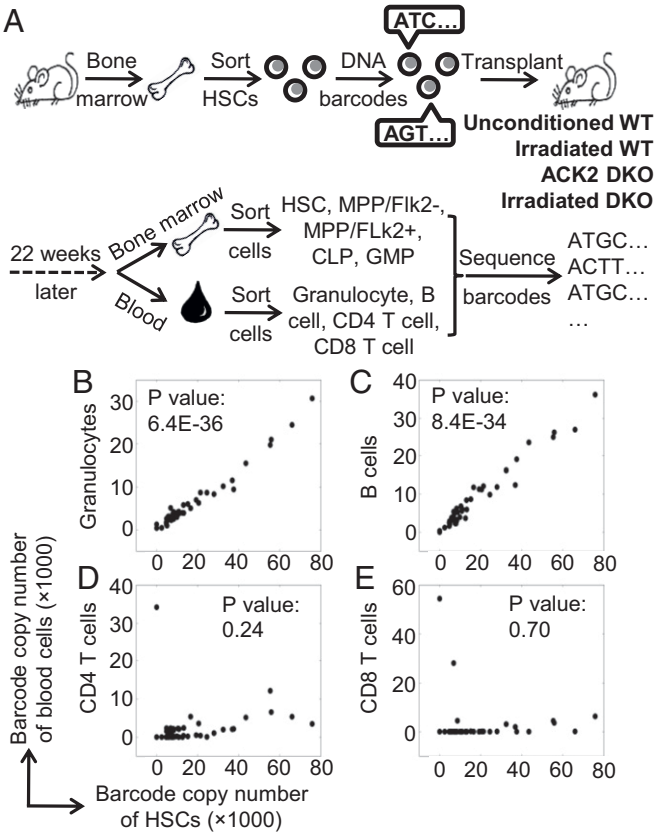

Fig. 1. Comparing clonality of HSCs with clonality of blood cells. (*A*) Experimental design. Donor HSCs are harvested from the bone marrow and genetically labeled with 33-bp barcodes using a lentiviral vector. Barcoded HSCs are transplanted into WT mice without any conditioning (unconditioned, $n = 8$), WT mice preconditioned with irradiation ($n = 7$), Rag2$^{-/-}\gamma c^{-/-}$ (DKO) mice preconditioned with anti-ckit antibody ($n = 7$), or DKO mice preconditioned with irradiation ($n = 10$). Twenty-two weeks after transplantation, donor-derived hematopoietic stem/progenitor cells [HSCs, Flk2– multipotent progenitor (MPP^{Flk2-}), Flk2+ multipotent progenitor (MPP^{Flk2+}), GMPs, CLPs], and mature blood cells (granulocyte, B cell, CD4 T cell, and CD8 T cell) are isolated from bone marrow and peripheral blood, respectively. Barcodes are extracted and analyzed as described elsewhere (37). (*B*–*E*) Barcode copy numbers from HSCs are compared with those from blood cells after unconditioned transplantation. Each dot represents a unique barcode that is used to track a single HSC clone. The *x* and *y* axes represent barcode copy numbers of different cell populations. The two-tailed *P* values of the Pearson correlation are shown to quantify the significance of the linear correlation. These scatter plots depict data from a single representative mouse. Data from all eight mice are shown in *SI Appendix*, Fig. S1.

barcode. As a donor-derived HSC differentiates through the various stages of lineage commitment after transplantation, we can obtain the copy numbers of its barcode from different cell populations at various differentiation stages. For example, the copy numbers of the same barcode can be measured in HSCs, granulocytes, B cells, and other cell populations. While the absolute copy number of a barcode from each cell population is influenced by the amount of barcoded DNA loaded onto the sequencer and the PCR amplification used to recover the barcode, the ratio of barcode copy numbers across different cell populations is informative. Equal ratios across different cell populations indicate that the respective clones expand at the same rate. However, dissimilar ratios indicate that some clones expand at a faster rate than the others.

The relative copy numbers of all barcodes from a population represent its "clonal composition." Comparing the clonal composition across various stages of differentiation, individual HSC clones can be mapped to precise lineages and stages of the hematopoietic hierarchy in a semiquantitative manner. This reveals the relative contributions of individual HSC clones to different hematopoietic lineages and their relative expansion during the stepwise lineage commitment process. As all cell populations were collected 22 weeks after transplantation, the data represent a snapshot of a dynamic hematopoiesis.

HSC Clones Homogenously Differentiate After Unconditioned Transplantation. Twenty-two weeks after unconditioned transplantation, all barcode copy number ratios of HSCs to granulocytes were approximately equal (Fig. 1*B* and *SI Appendix*, Fig. S1), indicating that every engrafted HSC clone expanded at a similar rate between these two stages. The same relationship held true for barcode copy numbers between the HSC and B cell stages (Fig. 1*C* and *SI Appendix*, Fig. S1). Taken together, the data indicate that donor-derived HSC clones homogenously contribute to granulocytes and B cells after unconditioned transplantation. However, not every HSC barcode could be found among CD4 T cells or CD8 T cells in the peripheral blood (Fig. 1 *D* and *E* and *SI Appendix*, Fig. S1), suggesting that some engrafted HSC clones do not contribute to the mature T cell repertoire. This could explain why a chronic myelocytic leukemia clone from the HSC pool can be found in granulocytes, monocytes, erythrocytes, and B cells but is rarely present in T cells (44). It is likely that the migration of the T cell precursors, mainly the common lymphocyte progenitors (CLPs), to the thymus or the maturation of T cells within the thymus is episodic and restricts the number of HSC clones that eventually contribute to mature T cells (45). Thus, it is important to use a specific blood-cell type, instead of all white blood cells, for HSC clonal tracking studies. Hence, in this study, we use granulocytes and B cells, both of which mature in the bone marrow, to analyze myeloid versus lymphoid lineage bias.

To determine how the clonal contribution of different HSCs evolves through the multiple stages of hematopoiesis, we examined the intermediate progenitors of myeloid and lymphoid differentiation (Fig. 2 *A* and *B* and *SI Appendix*, Fig. S2) (1–3). After unconditioned transplantation, the relative copy numbers of barcodes in HSCs remained generally constant in the multipotent progenitors, the oligopotent progenitors, and the terminally differentiated granulocytes and B cells (Fig. 2 *A* and *B* and *SI Appendix*, Fig. S2). This indicates a homogeneous clonal contribution of donor HSCs to the various stages of hematopoiesis. A few clones expanded at the progenitor stages, but this infrequent expansion was not reflected in blood cells (Fig. 2 *A* and *B* and *SI Appendix*, Fig. S2). Therefore, in unconditioned mice, HSC lineage commitment progresses with an equal contribution from each clone.

Pretransplantation Conditioning Induces Dominant Differentiation of HSC Clones. To compare HSC lineage commitment after unconditioned versus conditioned transplantation, identical numbers of barcoded HSCs were transplanted into unconditioned, lethally irradiated, or anti-ckit antibody (ACK2)-treated mice. As anti-ckit antibody conditioning was initially developed for facilitating HSC engraftment in severe combined immunodeficiency mice (26), ACK2 was studied in Rag2$^{-/-}\gamma c^{-/-}$ double-knockout (DKO) mice and control transplants using irradiation conditioning were also performed on the DKO mice. In contrast

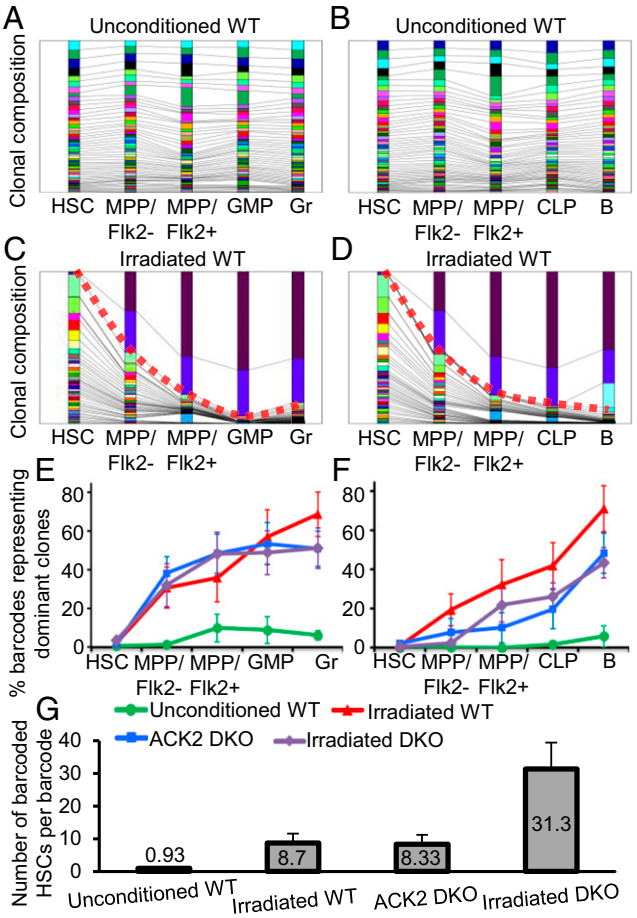

Fig. 2. Pretransplantation conditioning induces dominant differentiation of HSC clones. (*A–D*) Clonal compositions at each stage of HSC differentiation. Each column represents a hematopoietic population. Each colored section in a column represents one distinct genetic barcode, corresponding to an HSC clone. The size of each colored section indicates its relative abundance within each cell population. Identical barcodes from different cell populations (columns) are shown in the same color and are connected by lines. Red dotted lines highlight clones that exhibit dominant differentiation in irradiated mice. HSC, Flk2– multipotent progenitor (MPP^{Flk2-}), Flk2+ multipotent progenitor (MPP^{Flk2+}), GMP, CLP, granulocyte (Gr), and B cell (*B*) are arranged along myeloid differentiation stages (*A* and *C*) and lymphoid differentiation stages (*B* and *D*). Barcodes are arranged from top to bottom according to their abundances in terminally differentiated cells in the rightmost column of each panel. Shown are data from a WT recipient mouse not treated with any pretransplantation conditioning (*A* and *B*) and a WT recipient mouse treated with lethal irradiation before transplantation (*C* and *D*). Data from all eight unconditioned mice and seven irradiated mice are shown in *SI Appendix*, Fig. S2. (*E* and *F*) The percentage of barcodes representing dominant clones at each stage of HSC differentiation under various transplantation conditions. Dominant clones are defined as those whose relative copy numbers in blood cells (granulocytes or B cells) are more than five times their relative copy numbers in HSCs. Similar results are obtained when dominant clones are defined by different threshold values (*SI Appendix*, Fig. S3 *A* and *B*). ACK2, a clone of anti-ckit antibody; DKO, Rag2$^{-/-}\gamma c^{-/-}$ mice. (*G*) Number of harvested barcoded HSCs carrying the same barcode 22 wk after transplantation. GFP+ HSCs are counted as barcoded HSCs at the time of harvest, as GFP is constantly expressed in the barcode vectors. (*E–G*) Error bars show the SEMs for all mice under the same transplantation conditions.

to the homogeneous differentiation of all engrafted HSC clones in unconditioned mice (Fig. 2 *A* and *B* and *SI Appendix*, Fig. S2), in irradiated mice a small fraction of engrafted HSC clones expanded substantially faster than other clones during differentiation and supplied the majority of granulocytes and B cells (Fig. 2 *C* and *D* and *SI Appendix*, Fig. S2). We call this clonal behavior "dominant differentiation" and the clones that exhibit this behavior "dominant." It is important to note that dominant clones in irradiated mice are not dominant at the HSC stage but only become dominant at the intermediate progenitor stages as measured at week 22 posttransplantation (Fig. 2 *C* and *D* and *SI Appendix*, Fig. S2). In a conditioned mouse, more than half of the measured granulocytes and B cells descend from the dominant differentiation of a few HSC clones (Fig. 2 *E* and *F* and *SI Appendix*, Fig. S3 *A* and *B*). The dominant differentiation of HSC clones is present at similar levels after irradiation and ACK2 treatment (Fig. 2 *E* and *F* and *SI Appendix*, Fig. S3 *A* and *B*), indicating that it is not specific to either regimen, although this may also be influenced by the DKO setting.

While pretransplantation conditioning induced dominant clonal expansion in HSC differentiation, we asked whether it also influenced HSC self-renewal. At the time of transplantation, each barcode labels one HSC (37). If self-renewed, this HSC becomes multiple HSCs that all carry identical barcodes. Thus, the ratio of the number of HSCs to the number of unique barcodes increases with self-renewal. We found that after unconditioned transplantation each barcode was derived from about one barcoded HSC (Fig. 2*G*). This is very similar to the cell-to-barcode ratio of the original HSC infection (37). Therefore, donor-derived HSCs are not significantly amplified in recipient mice after unconditioned transplantation. This indicates that HSCs are not pressured to expand during homeostatic hematopoiesis after unconditioned transplantation in WT animals. In contrast, when the endogenous HSCs have been depleted by transplantation conditioning, donor HSCs must expand via self-renewal to reconstitute the entire HSC pool. Consistent with this prediction, after conditioned transplantation each barcode was derived from, on average, more than eight barcoded HSCs (Fig. 2*G*). Thus, HSCs had experienced at least three cell cycles of self-renewal by week 22 after conditioned transplantation. HSCs in irradiated DKO recipients exhibited a higher level of self-renewal than those in irradiated WT recipients. Therefore, it is unclear if the increased HSC self-renewal observed in ACK2-treated DKO recipients is due to the ACK2 treatment or the DKO setting. Nonetheless, HSCs dominantly expanded during self-renewal and differentiation in irradiated mice but not in unconditioned mice (Fig. 2).

Pretransplantation Conditioning Induces HSC Lineage Bias. The lineage bias of an HSC clone is determined by its relative contribution to myeloid versus lymphoid lineages. For example, HSC barcodes with myeloid bias have relatively high copy numbers in myeloid cell types such as granulocytes and relatively low copy numbers in lymphoid cell types such as B cells. After irradiation-mediated transplantation, donor-derived HSC clones were separated into three groups using the ratio of granulocyte barcode copy numbers to B cell barcode copy numbers (Fig. 3 *B* and *D* and *SI Appendix*, Fig. S4). These three groups represented myeloid bias, lymphoid bias, and lineage balance, consistent with previous studies (8, 10, 12, 13, 15). In ACK2-treated mice, HSC clones also exhibited both lineage biases and lineage balance, forming three clearly separated groups (Fig. 3*C* and *SI Appendix*, Fig. S4). The fraction of HSCs exhibiting lineage bias and balance was similar after irradiation and after ACK2 treatment (*SI Appendix*, Fig. S3*C*). However, no lineage bias was observed when pretransplantation conditioning was absent (Fig. 3*A* and *SI Appendix*, Fig. S4).

The lineage bias and balance of engrafted clones are also affected by the irradiation dosage and by the number of helper cells used in the transplantation procedure (Fig. 3*E*). Compared with lethal irradiation, increasing the number of helper cells resulted in significantly fewer myeloid-biased clones (Fig. 3*E*). However, half-lethal irradiation produced significantly fewer lymphoid-biased clones (Fig. 3*E*). The use of more helper cells and the reduction of the irradiation dosage both generated significantly more balanced HSC clones (Fig. 3*E*). Thus, the observed lineage bias of donor HSCs is highly sensitive to transplantation conditions and is absent when no conditioning regimen is applied (Fig. 3).

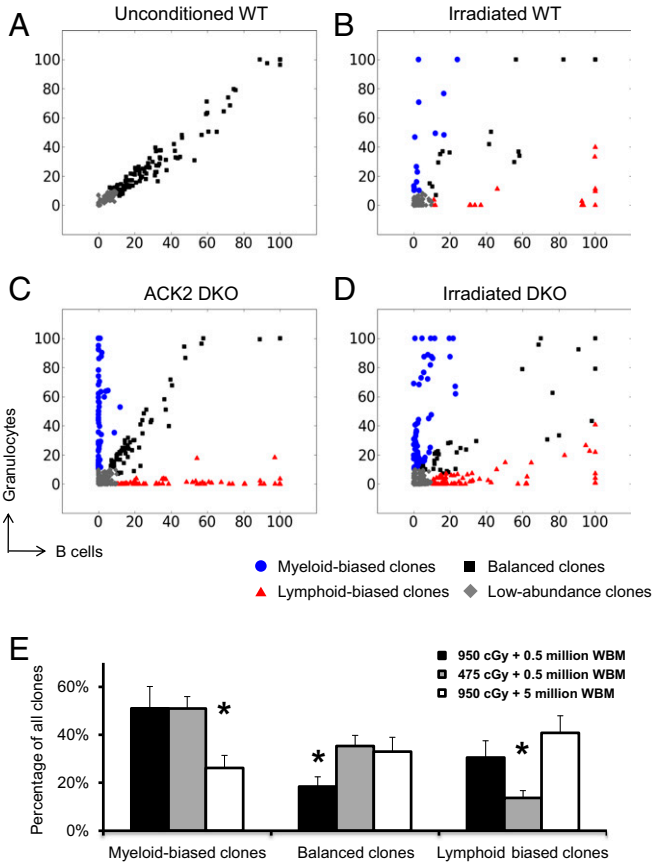

Fig. 3. Pretransplantation conditioning induces HSC lineage bias. (*A–D*) Scatter plots comparing barcode copy numbers from granulocytes with barcode copy numbers from B cells in the peripheral blood. Each dot represents a unique barcode that is used to track a single HSC clone. Colors are assigned according to the ratios of the granulocytes' barcode copy numbers (myeloid lineage) to B cells' barcode copy numbers (lymphoid lineage). Lineage-biased clones are defined as those whose relative copy numbers in one lineage are more than 2.4142 (cotangent 22.5°) times their relative copy numbers in the other lineage. Low-abundance clones are excluded from the analysis of lineage bias versus balance. These clones are defined as those whose copy numbers are less than 10% of the maximum copy numbers in both lineages. Shown are the barcodes from all mice examined under each condition. Barcode copy numbers are normalized to the most abundant clone in each cell population of each mouse. Mice with insufficient reads (maximum barcode copy number <5,000) or with a low number of barcodes (fewer than three unique barcodes present in granulocytes and B cells) are excluded from these plots. Raw data from all mice are shown individually in *SI Appendix*, Fig. S4. The percentages of barcodes with distinct lineage bias and balance are summarized in *SI Appendix*, Fig. S3C. (*E*) Lineage bias and balance of donor HSCs after various conditions of irradiation-mediated transplantations. Shown are percentages of clones with distinct lineage bias or balance. Lethal irradiation uses 950 cGy and 0.5 million helper cells (whole bone marrow cells, WBM). Half-lethal irradiation uses 475 cGy and 0.5 million helper cells. The "more helper cells" condition uses 5 million helper cells and 950 cGy. Error bars show the SEMs for all mice under the same transplantation conditions. *$P < 0.05$ by Student's t test.

Dominant Differentiation and Lineage Bias Are Connected. As dominant differentiation and lineage bias are both present in conditioned recipients and both absent in unconditioned recipients, we wondered whether they are associated with each other and simultaneously affect the same HSC clones. We separated all HSC clones of conditioned recipients into dominant and nondominant groups based on their expansion between HSCs and blood cells (including both granulocytes and B cells). We then examined the lineage bias and balance of each group. In irradiated mice, both dominant clones and nondominant clones exhibited similar proportions of lineage bias and balance (Fig. 4 *A* and *C* and *SI Appendix*, Fig. S5). However, in ACK2-treated mice, dominant clones exhibited lineage bias, whereas nondominant clones exhibited lineage balance (Fig. 4*B* and *SI Appendix*, Fig. S5). In these mice, if dominant clones were excluded, the remaining clones were mostly balanced, as if they had been transplanted without any conditioning (Fig. 4*D*). This suggests that HSC differentiation regulatory mechanisms, active under normal homeostatic conditions, are still active in ACK2-treated mice and regulate a subset of engrafted HSC clones. However, these mechanisms are inactivated in irradiated mice. The concurrence of dominant differentiation and lineage bias in HSC clones of ACK2-treated mice indicates a connection between these two phenotypes (Fig. 4*B* and *SI Appendix*, Fig. S5).

Lineage bias is associated with clonal expansion not only during HSC differentiation (Fig. 4*B*) but also during HSC self-renewal (Fig. 4*E*). In ACK2-treated mice, balanced HSC clones underwent significantly more self-renewal than other clones in the same mice and the clones in irradiated mice during the first 22 wk after transplantation (Fig. 4*E*). This suggests that balanced clones preferentially self-renew in ACK2-treated mice. Thus, a clonal competition appears to exist in these mice where lineage-balanced clones outcompete lineage-biased clones in numbers at the HSC stage. Taken together, these data suggest a connection between lineage bias, lineage commitment, and self-renewal in ACK2-treated mice, where lineage-biased clones dominantly expand at specific steps of lineage commitment and exhibit low self-renewal (Fig. 4).

Lineage Bias Arises from Dominant Differentiation at Distinct Lineage Commitment Steps. As lineage bias is associated with dominant differentiation (Fig. 4 and *SI Appendix*, Fig. S5), we asked whether lineage bias is derived from the dominant differentiation of any particular lineage commitment steps. We examined the percentage of barcodes representing myeloid-biased clones at various stages of myeloid differentiation and found that the greatest expansion of myeloid-biased barcodes occurred between the HSC and Flk2− multipotent progenitor (MPP^{Flk2-}) stages (Fig. 5*A* and *SI Appendix*, Fig. S6). In contrast, lymphoid-biased clones underwent the greatest expansion at the last lineage commitment step from CLP to B cell (Fig. 5*A* and *SI Appendix*, Fig. S6). These patterns were found in both ACK2-treated mice and irradiated mice (Fig. 5*A*). In addition, if we examined all clones that expanded dominantly at the CLP-to-B-cell step, they were significantly more likely to end up with lymphoid bias in both ACK2-treated mice and irradiated mice (Fig. 5*B*). However, clones that expanded dominantly at the HSC-to-MPP^{Flk2-} step were significantly more likely to develop myeloid bias in ACK2-treated mice (Fig. 5*B*). However, in irradiated mice, these clones became either myeloid-biased or balanced (Fig. 5*B*). This indicates that balanced clones in irradiated mice also dominantly differentiate, which will be discussed in depth later (Fig. 6 *A* and *B*). Taken together, these data suggest that myeloid versus lymphoid lineage bias arises from dominant differentiation at distinct lineage commitment steps (Fig. 5 *A* and *B*).

If myeloid bias arises at the first differentiation step and lymphoid bias arises at the last differentiation step, as in the case of ACK2-treated mice (Fig. 5 *A* and *B*), then myeloid bias but not lymphoid bias should characterize the intermediate progenitor stages. This is validated by data from granulocyte/monocyte progenitors (GMPs) and CLPs (Fig. 5 *C* and *D*). In ACK2-treated mice, clones with myeloid bias at the progenitor stages significantly preserved their myeloid bias in blood cells (Fig. 5 *C* and *D*). Moreover, lymphoid-biased clones and balanced clones at the progenitor stages did not preserve their bias and balance in blood cells, which is consistent with the prediction (Fig. 5 *C* and *D*). In irradiated WT mice, all of the clones appeared to be balanced at the progenitor stages (Fig. 5*D*). In contrast, when $Rag2^{-/-}\gamma c^{-/-}$ (DKO) mice lacking mature lymphoid cells were used as irradiation

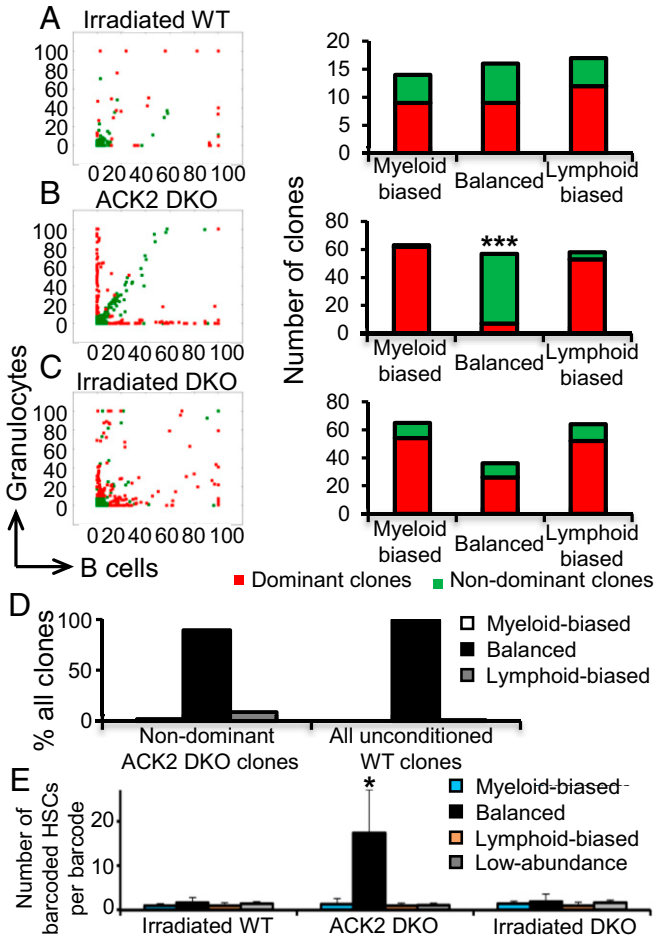

Fig. 4. Connections between dominant differentiation and lineage bias. (*A*–*C*) Dominant clones and nondominant clones are compared by their lineage bias and balance. (*A*–*C*, *Left*) Plots are generated as described in the legend for Fig. 3 *A*–*D*. Colors are assigned according to the ratios of HSC barcode copy numbers to granulocytes and B cells copy numbers. Dominant clones are defined as those whose relative copy numbers in blood cells (granulocytes or B cells) are more than five times their relative copy numbers in HSCs. Similar results are obtained when dominant clones are defined by different threshold values (*SI Appendix*, Fig. S5). (*A*–*C*, *Right*) The number of clones with lineage bias or balance from all mice under the indicated transplantation condition. *P* value depicts the probability that a given result is caused by dominant or nondominant clones randomly becoming lineage-biased or balanced. (*D*) Lineage bias and balance of nondominant clones in ACK2-treated $Rag2^{-/-}\gamma c^{-/-}$ mice (DKO) compared with all clones in unconditioned WT mice. (*E*) Numbers of lineage-biased or balanced barcoded HSCs carrying the same barcode. Data are normalized by lymphoid-biased barcodes of each transplantation condition. GFP+ HSCs are counted as barcoded HSCs at the time of harvest, as GFP is constantly expressed in the barcode vectors. Error bars show the SEMs for all mice under the same transplantation conditions. $*P < 0.05$ by Student's *t* test, $***P < 0.001$.

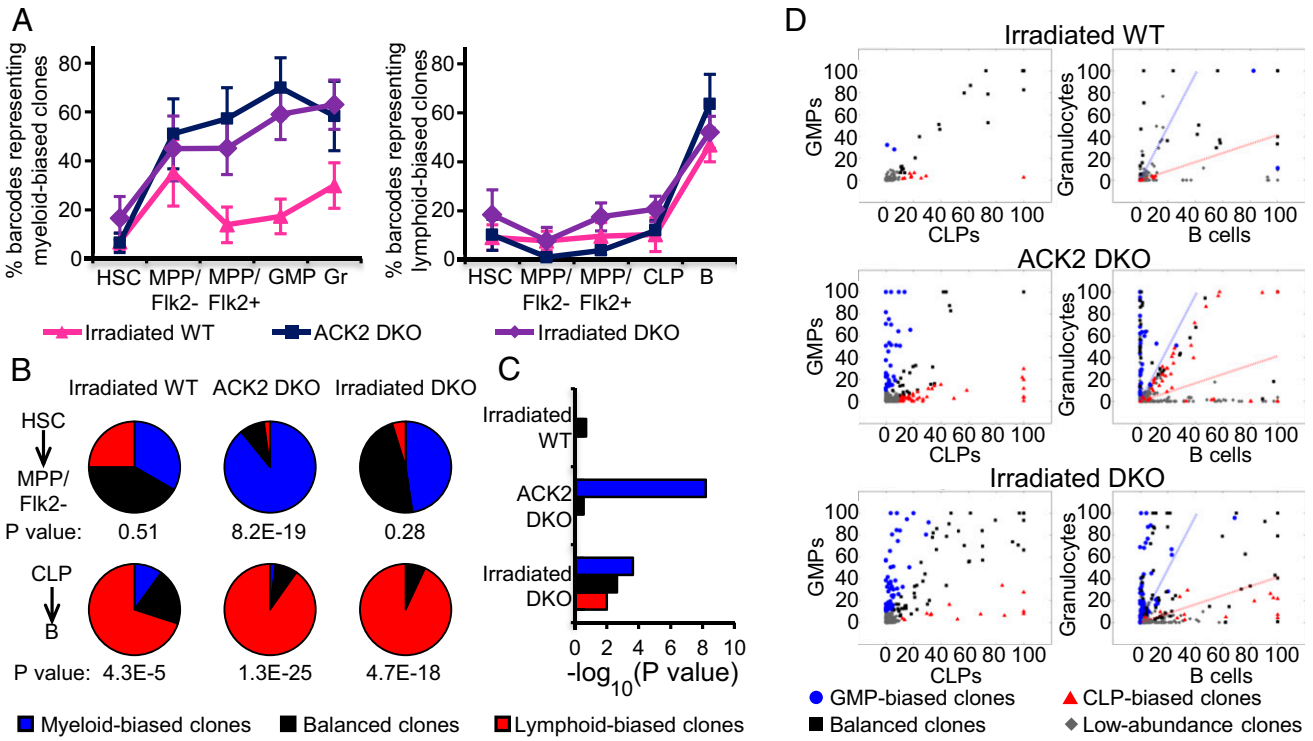

Fig. 5. Lineage bias of HSCs is derived from dominant differentiation at distinct lineage commitment steps. (*A*) Plots were generated as described in the legend for Fig. 2 *E* and *F*, except that only myeloid-biased clones (*Left*) or lymphoid-biased clones (*Right*) are plotted. Other clones are shown in *SI Appendix*, Fig. S6. (*B*) Pie charts illustrate the lineage bias and balance of the clones that expand dominantly from HSC to MPP^{Flk2-} (*Upper*) or from CLP to B cells (*Lower*). *P* value depicts the significance that the clones that dominantly expand during HSC-to-MPP^{Flk2-} commitment become myeloid-biased (*Upper*) and that the clones that dominantly expand during CLP-to-B-cell commitment become lymphoid-biased (*Lower*). (*C*) *P* value depicts the significance that the lineage bias and balance at the progenitor stages is reflected in blood cells. (*B* and *C*) *P* value is calculated to quantify the probability that the clones are randomly distributed among the different categories of lineage bias and balance. (*D*) Plots are generated as described in the legend for Fig. 3 *A*–*D*. Dot colors in all plots are assigned based on the bias between GMPs and CLPs. The dotted lines show the boundary of lineage bias versus balance in blood cells. Analysis based on the lineage bias exhibited in blood cells is shown in *SI Appendix*, Fig. S7, where dot colors are assigned based on the bias between granulocytes and B cells.

recipients, the progenitors exhibited lineage bias (Fig. 5*D*). This bias was moderately preserved in blood cells (Fig. 5*C*), which will be discussed in depth later (Fig. 6 *E* and *F*). These data suggest that when transplantation recipients are lineage-deficient, lineage bias could be determined upstream of the oligopotent progenitors.

Lineage Commitment Profiles of HSC Clones with Distinct Lineage Bias and Balance. To systematically examine the lineage commitment paths that lead to differential blood production, we analyzed the average abundance of clones with distinct lineage bias and balance through various stages of lineage commitment (Fig. 6). In ACK2-treated DKO mice, myeloid-biased clones expanded dominantly between the HSC and MPP^{Flk2-} stages (Figs. 5*A* and 6*C*). These clones were diminished at the CLP and B cell stages (Fig. 6*D*). In contrast, lymphoid-biased clones expanded dominantly between the CLP and B cell stages (Figs. 5*A* and 6*D*), and their abundances remained low during the initial lineage commitment and the myeloid lineage commitment stages (Fig. 6*C*). Balanced HSC clones did not exhibit dominant differentiation in either lineage (Fig. 6 *C* and *D*), consistent with previous analysis (Fig. 4*B* and *SI Appendix*, Fig. S5). The fluctuations of the balanced clones appear to be inversely correlated with the dominant differentiation of myeloid-biased clones and lymphoid-biased clones (Fig. 6 *C* and *D*), indicating that the fluctuation is probably not a real change but is rather a reflection of the dominant expansion of other clones. This can be attributed to the data normalization procedure that normalizes the total abundance of all barcodes in each cell population to 100%. Interestingly, these balanced clones were more abundant at the HSC stage than other clones (Figs. 4*E* and 6 *C* and *D*). The high abundances persisted in their downstream progenies (Fig. 6 *C* and *D*), suggesting that balanced clones are significantly more committed to self-renewal than other clones, and that all self-renewed, balanced HSCs differentiate.

In irradiated WT mice, lineage-biased and balanced clones all exhibited similar abundances at the HSC stage (Fig. 6 *A* and *B*). Myeloid-biased clones dominantly expanded twice during the lineage commitment process (Fig. 6*A*). The first dominant expansion occurred between the HSC and MPP^{Flk2-} stages and the second dominant expansion occurred between the GMP and granulocyte stages (Fig. 6*A*). There was a reduction between these two expansions, and irradiated WT mice did not exhibit lineage bias at the progenitor stages (Fig. 5*D*). Myeloid-biased clones did not expand between the CLP and B cell stages, whereas lymphoid-biased clones expanded dominantly at this lineage commitment step (Figs. 5*A* and 6*B*). Lymphoid-biased clones did not dominantly expand at any other lineage commitment steps, but they were more abundant than undifferentiated clones at the MPP and CLP stages, suggesting that lymphoid-biased clones are not absent during the early stages of lymphoid differentiation (Fig. 6 *A* and *B*). Most strikingly, balanced clones dramatically expanded in irradiated mice at almost every lineage commitment step (Fig. 6 *A* and *B*). Their relatively less severe expansion at the last step, the GMP-to-granulocyte step, and the CLP-to-B-cell step, is likely a reflection of the dominant differentiation

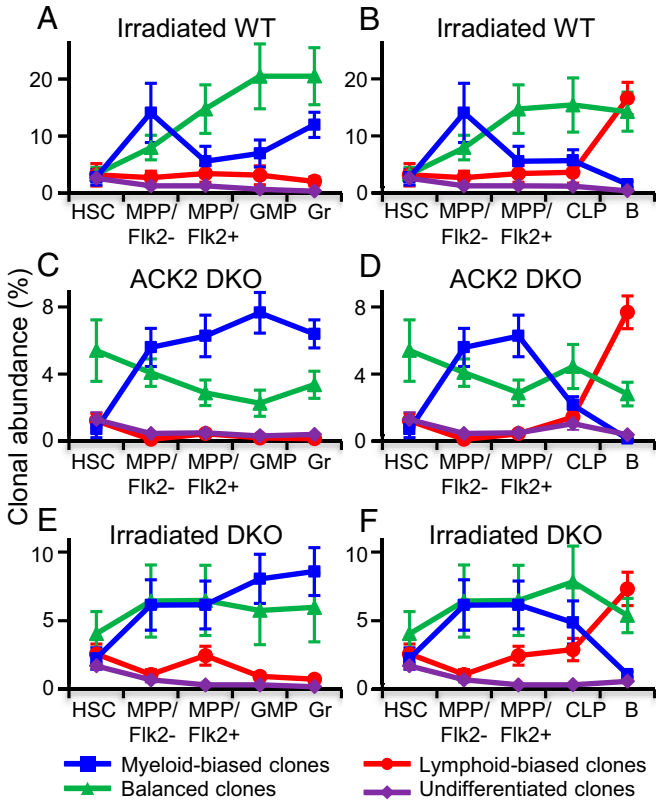

Fig. 6. Lineage commitment of HSC clones with distinct lineage bias and lineage balance. Shown are the average abundance of clones with distinct lineage bias and balance at various stages of HSC differentiation. Clonal abundance here refers to the copy number of a particular barcode as a percentage of all barcode copy numbers from a cell population. (*A* and *B*) Irradiated WT mice. (*C* and *D*) ACK2-treated Rag2$^{-/-}\gamma c^{-/-}$ mice. (*E* and *F*) Irradiated Rag2$^{-/-}\gamma c^{-/-}$ mice. (*A*, *C*, and *E*) Myeloid differentiation toward granulocytes. (*B*, *D*, and *F*) Lymphoid differentiation toward B cells. Error bars show the SEMss for all of the barcodes from mice under the same transplantation conditions. DKO, Rag2$^{-/-}\gamma c^{-/-}$ mice.

of myeloid-biased clones and lymphoid-biased clones, due to data normalization (Fig. 6 *A* and *B*).

In irradiated DKO mice, balanced clones exhibited moderate expansion during self-renewal and differentiation (Fig. 6 *E* and *F*), a phenotype in between that of ACK2-treated DKO mice and irradiated WT mice (Fig. 6 *A*–*D*). Myeloid-biased clones and lymphoid-biased clones in irradiated DKO mice (Fig. 6 *E* and *F*) exhibited lineage commitment profiles similar to those in ACK2-treated DKO mice (Fig. 6 *C* and *D*), combining characteristics from irradiated WT mice (Fig. 6 *A* and *B*) such as the double expansion of myeloid-biased clones. The second expansion of myeloid-biased clones occurred not at the last lineage commitment step but at the MPP^{Flk2+}-to-GMP step. In addition, lymphoid-biased clones also started to expand early at the MPP^{Flk2-}-to-MPP^{Flk2+} step (Fig. 6 *E* and *F*). The early expansion of lineage-biased clones in irradiated DKO mice may have been related to the ubiquitous expansion of all differentiating clones observed in irradiated WT mice and to the DKO setting. Taken together, the comparison of irradiated DKO mice and ACK2-treated DKO mice manifests the characteristics of irradiation-mediated transplantation observed in WT mice as well.

Discussion

In this study, we identify the clonal-level lineage commitment pathways of HSCs in vivo. Under various transplantation conditions, we show that lineage commitment of HSC clones after conditioning is characterized by dominant differentiation and lineage bias (Figs. 2 and 3). In addition, we show that dominant differentiation and lineage bias are interrelated (Figs. 4 and 5) and together delineate distinct pathways that lead to balanced or biased blood production (Fig. 6). These pathways elucidate cellular proliferation and differentiation of HSCs at the clonal level and demonstrate distinct modes of HSC regulation in vivo.

A Model of Clonal-Level Lineage Commitment Pathways of HSCs in Vivo. Based on all of the data (Figs. 1–6), we propose a model for the clonal-level lineage commitment pathways of HSCs in vivo (Fig. 7). After unconditioned transplantation, all engrafted HSCs uniformly differentiate and self-renew (Figs. 1 *B* and *C* and 2 *A*, *B*, and *G*). While they may contribute differently to blood cells with distinct maturation processes, such as T cells (Fig. 1 *D* and *E*), they do not exhibit dominant differentiation or myeloid versus lymphoid lineage bias (Figs. 2 and 3). In contrast, after conditioned transplantation, only a small subset of engrafted HSC clones are involved in differentiation (Fig. 2 *C*–*F*). These clones follow distinct pathways that are characterized by dominant differentiation and lineage bias.

After ACK2 antibody-mediated transplantation in DKO mice, differentiating HSC clones follow one of three pathways (Fig. 7). In the first pathway, the majority of HSC clones do not exhibit dominant differentiation or lineage bias (Fig. 4*B*). Their lineage commitment process resembles that of HSC clones transplanted into unconditioned recipients (Fig. 4*D*). Furthermore, these HSC clones self-renew significantly more than other HSC clones (Figs. 4*E* and 6 *C* and *D*). In the second pathway, HSC clones dominantly expand at the first lineage commitment step, HSC to MPP^{Flk2-} (Fig. 5*A*). These HSC clones eventually become myeloid-biased (Fig. 5*B*), which may be triggered by the ACK2-mediated depletion of host myeloid progenitors (26). In the third pathway, HSC clones dominantly expand at the last lineage commitment step, CLP to B cell (Fig. 5*A*), and end up with lymphoid bias (Fig. 5*B*), which may be in part due to the DKO setting. Additionally, other HSC clones are not recruited into differentiation and do not participate in any of these pathways but instead remain quiescent and can be found even at 22 weeks after transplantation (Fig. 6 *C* and *D* and *SI Appendix*, Fig. S6 *E* and *F*).

After irradiation-mediated transplantation, HSC clones follow lineage commitment pathways similar to those after

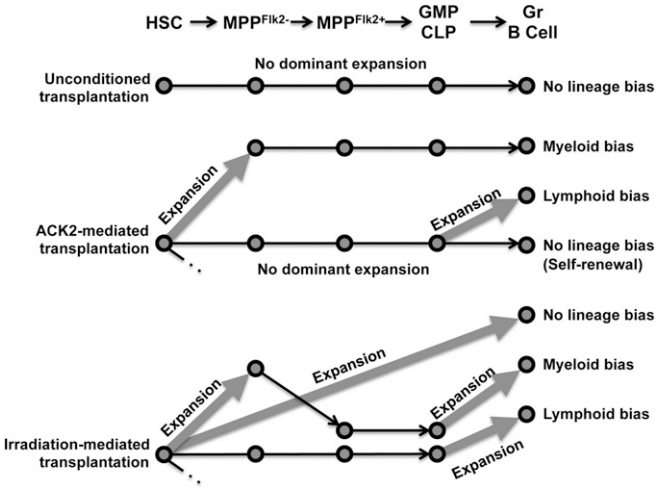

Fig. 7. A model of clonal-level lineage commitment pathways of HSCs in vivo. Thicker and ascendant arrows represent dominant differentiation of HSC clones. HSCs transplanted into mice pretreated with different conditioning regimens follow distinct pathways during lineage commitment. These pathways lead to distinct balanced or biased blood production.

ACK2-mediated transplantation (Fig. 7). The major difference is that all differentiating HSCs dominantly expand during differentiation in irradiated recipients regardless of their lineage bias or balance (Fig. 6 *A* and *B*). This dominant expansion is manifested in distinct differentiation lineages and stages in different pathways. However, none of these pathways is associated with dominant self-renewal (Figs. 4*E* and 6 *A* and *B*). In particular, balanced HSCs expand dramatically at every step of the lineage commitment process (Fig. 6 *A* and *B*). The dominant differentiation of balanced clones may restrain the expansion of myeloid-biased clones, such that myeloid-biased clones are not significantly more present in GMP than lymphoid-biased clones (Fig. 6*A*). Therefore, lineage bias is absent at the GMP and CLP stages in WT irradiated recipients (Fig. 5*D*). The MPP^{Flk2-} population has recently been found to contain two MPP subsets (MPP2/3) that represent distinct pathways of differentiation (29). The observed clonal expansion in MPP^{Flk2-} may be associated with a subset of this population. Downstream of these progenitors, myeloid-biased clones expand again at the last step of lineage commitment from GMP to granulocyte. Lymphoid-biased and undifferentiated pathways in irradiated recipients exhibit lineage commitment characteristics similar to their counterparts in ACK2-treated recipients (Figs. 5 *A* and *B* and 6).

Transplantation Conditions Alter HSC Differentiation at the Clonal Level. Irradiation is used in the vast majority of HSC studies. It is also widely applied in clinical therapies to facilitate bone marrow transplantation and to treat cancers and hematopoietic disorders. Here, we have shown how irradiation alters HSC regulation at the clonal level (Figs. 2 and 3). This striking alteration could lead to new interpretations of HSC physiology studies that use irradiation as a conditioning regimen. For example, many recent studies propose that HSCs are heterogeneous and possess differential lineage bias (8, 10, 12, 13, 15). These studies all used irradiation to facilitate HSC engraftment. Our data now demonstrate that engrafted HSCs uniformly differentiate and self-renew in the absence of any pretransplantation conditioning and that heterogeneous hematopoiesis is only observed after conditioned transplantation (Figs. 2 and 3). This indicates that the conditioning regimen used in the previous studies may have contributed to the observed HSC heterogeneity. Thus, future studies must be carefully designed to distinguish normal HSC physiology from emergency modes.

HSC regulatory mechanisms activated after conditioning are likely to be more susceptible to perturbation and damage (46). These mechanisms may be key to understanding how hematopoiesis becomes malignant and to reducing the side effects of clinical regimens used to treat these malignancies. For example, during several gene therapy trials, researchers were dismayed by the appearance of clonal dominance in the blood cells of treated patients (47, 48). This clonal dominance was interpreted to be a result of viral integration that ectopically activated nearby oncogenes and drove cellular expansion. However, our data suggest that the observed clonal dominance may instead have been induced by the use of pretransplantation conditioning regimens that accompanied the gene therapy procedure. Optimal regeneration of gene-modified HSCs may emerge by testing acceptable conditioning conditions in preclinical nonhuman primate studies and clinical trials.

In addition to irradiation conditioning, we showed that ACK2-mediated transplantation alters HSC differentiation to a lesser extent (Figs. 2–7). Both conditioning regimens interrupt homeostatic hematopoiesis and trigger emergent demands for hematopoietic cells, which may induce the observed clonal expansion and lineage bias. The more profound effect of irradiation may drive the higher levels of clonal expansion and lineage bias in HSC differentiation, which could be associated with its increased damage to the niche. Interestingly, cotransplantation of differing numbers of transient progenitor (helper) cells was found to change donor HSC differentiation, further suggestive of a need-sensing mechanism (Fig. 3*E*). Additionally, recent work in our laboratory has shown how HSC differentiation is influenced by the amount of donor HSCs (38) and by the presence of defective HSCs (39). Taken together, these findings suggest that HSC self-renewal and differentiation programs can be altered by transplantation conditions and by environmental conditions and demands.

Cellular Origins of Clonal Dominance and Lineage Bias. Our elucidation of the HSC clonal-level lineage commitment pathways reveals the HSC regulatory mechanisms and identifies the cellular origins of the clonal dominance and lineage bias that were previously observed in blood cells (8, 10, 12, 13, 15). Recent studies suggested that HSCs differentiate through different MPP subsets and produce distinct lineage biases (17, 29, 42, 49). Our study showed that most HSC clones were found in both MPP^{Flk2-} and MPP^{Flk2+} subsets (Fig. 2). In particular, clonal dominance is initiated by the outgrowth of clones predominantly at the hematopoietic progenitor stages, and not at the HSC stage (Fig. 2). This explains why previous studies detected few clones in the blood after irradiation (11, 40, 41, 50). We demonstrate that lineage bias arises from the dominant clonal expansion of specific lineages at key lineage commitment steps in conditioned mice (Fig. 5) and explains the presence of lineage bias in blood (8, 10, 12, 13, 15). Dominant clonal expansion may arise from high-performing clones, perhaps in response to the poor performance of other clones.

Unconditioned Transplantation Provides Unique Insights into Natural HSC Physiology. Unconditioned transplantation minimally perturbs natural hematopoiesis and provides insights into natural HSC physiology and additionally provides insights into unconditioned lentiviral gene therapy studies (51). In our studies, we did not detect the presence of "dormant HSCs" (52) in unconditioned transplantation (Figs. 1 *B* and *C* and 2 *A* and *B*). It is possible that "active HSCs" are selectively engrafted or that HSCs engrafted after unconditioned transplantation are regulated as active HSCs and not as dormant HSCs. While our unconditioned transplantation is limited to analyzing engrafted HSCs, recent studies using transposon tagging bone marrow cells suggest that some HSC clones preferentially differentiate into the megakaryocyte lineage during native hematopoiesis (16, 17). Nonetheless, our data suggest that engrafted HSCs continuously and homogenously contribute to the blood pool (Figs. 1 *B* and *C* and 2 *A* and *B*). As HSCs frequently migrate through the peripheral blood and reenter their niche under homeostatic conditions (34–36), this process may be a natural procedure to select for active and lineage-balanced HSCs (Figs. 1 *B* and *C* and 2 *A* and *B*). The homogeneity of HSC clonal behavior indicates that HSCs can be uniformly regulated in their niche and do not require a complex regulatory system to shepherd selected HSCs in and out of differentiation and self-renewal under homeostatic conditions (11, 40, 41, 53).

Different Clonal Pathways Can Coexist Simultaneously in a Single Organism. By tracking many HSC clones simultaneously after transplantation we identified several distinct pathways coexisting in a single mouse after conditioning (Fig. 7). These pathways mutually compensate to sustain overall blood and immune production (Figs. 6 and 7). Importantly, the striking differences in HSC regulation uncovered by this clonal analysis are not evident at the population level, further highlighting the importance of this type of assessment. This is not unexpected, as blood cells are critical for the survival of the organism. Redundant and feedback mechanisms may have evolved to maintain overall blood production (2, 54).

An unexpected coexistence of different clonal pathways is found in ACK2-treated mice (Figs. 4 *B* and *D* and 7). In these

mice, one pathway preserves the characteristics from the unconditioned state, lacking both dominant differentiation and lineage bias. The other pathways resemble those from the irradiated state, exhibiting both dominant differentiation and linage bias, which may be due to sensing and filling the hematopoietic void created by the ACK2 treatment or due to niche injury. Interestingly, despite their differences in mechanism and toxicity, irradiation and ACK2 treatments both produce dominant differentiation and lineage bias (Figs. 2 and 3 and *SI Appendix*, Fig. S3*C*). The presence of the unconditioned pathway even after conditioning may be responsible for the long-term stability of hematopoiesis observed in clinical HSC transplantation, which is thought to be improved with nonablative conditioning (55, 56). The coexistence of the unconditioned pathway with pathways activated after conditioning in the same mouse suggests that these pathways are not mutually exclusive and are not altered by globally mobilized factors. It also provides the possibility for activating the unconditioned pathway in myeloablated (irradiated) patients as part of a therapeutic procedure to achieve benefits similar to that of less-myeloablated protocols.

Molecular Mechanisms Underlying the Lineage Commitment Pathways of HSC Clones. It would be clinically valuable to drive HSC differentiation into one particular lineage commitment pathway. However, the molecular mechanisms that determine how HSCs choose between the lineage commitment pathways are complex (Fig. 7) and likely involve both intrinsic and extrinsic factors. Several recent studies have revealed cell-surface markers on HSCs that enrich for distinct lineage bias shown when transplanted into irradiated hosts (8, 12, 15, 57). This suggests that select HSCs preferentially follow certain pathways. For example, the myeloid-biased HSC clones are enriched with $CD150^{hi}$, and the balanced clones are enriched with $CD150^{med}$ (8, 12, 15), showing that the predisposition for clonotypes is determined at the HSC level but read out at the level of different progenitors. It has also been shown that cytokines can direct hematopoiesis into distinct lineages (4–7), which suggests that extrinsic factors can alter the pathway choices of HSCs.

HSCs in conditioned and unconditioned recipients may receive different regulatory signals (Figs. 2 and 3). These signals may selectively engraft a subset of HSCs that are lineage-biased and may induce lineage bias from balanced HSCs. In the latter scenario, it is possible that intrinsic differences among HSCs elicit different responses to the conditioning regimen (2, 8, 57). These regulatory signals may be produced as a consequence of stimulation or damage to the HSC niche by the conditioning regimen (28). A blood cell deficiency may also induce feedback signals that boost HSC differentiation. These signals can activate the first few HSCs landing at niches and instruct them to dominantly differentiate to compensate for the hematopoietic deficiency. We have shown that, after irradiation, all differentiating HSC clones expand dominantly at various stages (Figs. 6 *A* and *B* and 7), indicating the stress for the HSCs to supply the blood cells after irradiation.

In summary, we have provided a comprehensive view of HSC lineage commitment at the clonal level after transplantation and have uncovered the underlying lineage commitment pathways of individual HSC clones (Fig. 7). These pathways are altered by transplantation conditioning such as irradiation (Figs. 2 and 3), which has been ubiquitously used in HSC studies. The pathways also identify the HSC differentiation stages where HSC clones become dominant and where lineage bias originates (Figs. 5 and 6). These studies reveal important insights into the diversity of HSC behavior and provide opportunities for studying the underlying regulatory mechanisms. In addition to improving understanding of hematopoiesis, knowledge of clonal-level HSC lineage commitment pathways opens new avenues of research for understanding and manipulating blood production and balance, understanding potential malignant evolution, and improving transplantation treatments.

Experimental Procedures

The donor mice used in all experiments were C57BL6/K_a ($CD45.1^+$). The recipient mice used in the unconditioned transplantation experiments (M1–8) were C57BL6/K_a ($CD45.1^+/CD45.2^+$). The recipient mice used in the irradiation-mediated transplantation experiments (M9–15, and those used in Fig. 3*E*) were C57B L6/K_a ($CD45.2^+$). The recipient mice used in the ACK2-mediated transplantation experiments (M16–22) were $Rag2^{-/-}\gamma c^{-/-}$ with C57BL6/K_a background (DKO) (26). The DKO mice were also used as irradiation recipients (M23–32). All donor and recipient mice were 8 to 12 wk old at the time of transplantation. Mice were bred and maintained at Stanford University's Research Animal Facility. Animal procedures were approved by the Institutional Animal Care and Use Committee.

HSCs [lineage (CD3, CD4, CD8, B220, Gr1, Mac1, Ter119)$^-$/ckit$^+$/Sca1$^+$/Flk2$^-$/CD34$^-$/CD150$^+$] were obtained from the crushed bones of donor mice and isolated using double FACS sorting with the FACS-Aria II (BD Biosciences) after enrichment using CD117 microbeads (AutoMACS; Miltenyi Biotec). HSCs were infected for 10 hours with lentivirus carrying barcodes and then transplanted via retroorbital injection. Recipient mice were treated with one of the following three conditions before transplantation: (*i*) no treatment, referred to as "unconditioned" (M1–8), (*ii*) irradiation with 950 cGy immediately before transplantation (M9–15 and M23–32), or (*iii*) retroorbital injection of 500 μg of ACK2 into $Rag2^{-/-}\gamma c^{-/-}$ mice 9 days before transplantation (26) (M16–22). In unconditioned transplantation, 1,000 barcoded HSCs were transplanted into each mouse every other day for 18 days (9,000 donor HSCs total). Long-term stable engraftment of ∼1% donor chimerism was consistently obtained. In irradiation-mediated and ACK2-mediated transplantation, 9,000 donor HSCs were transplanted all at once. Donor chimerism observed in granulocytes was around 90% and 10%, respectively; 250,000 whole bone marrow cells without viral transduction were cotransplanted into each irradiated mouse as helper cells, except specified otherwise (Fig. 3*E*). All cells were harvested 22 weeks after transplantation.

HSC clonal labeling and data analysis are explained in detail elsewhere (37). Dominant clones are defined as those whose relative copy numbers in blood cells are more than five times their relative copy numbers in HSCs. Lineage-biased clones are defined as those whose relative copy numbers in one lineage are more than 2.4142 (cotangent 22.5°) times their relative copy numbers in the other lineage. Low-abundance clones are excluded from the analysis of lineage bias versus balance. These clones are defined as those whose copy numbers are less than 10% of the maximum copy numbers in both lineages. All results have been reaffirmed using different lineage bias and clonal dominance threshold values.

Below is the list of cell-surface markers used to harvest hematopoietic populations. Donor cells were sorted based on the CD45 marker.

Granulocytes: CD4$^-$/CD8$^-$/B220$^-$/CD19$^-$/Mac1$^+$/Gr1$^+$/side scatter^{high};

B cells: CD4$^-$/CD8$^-$/Gr1$^-$/Mac1$^-$/B220$^+$/CD19$^+$;

CD4 T cells: B220$^-$/CD19$^-$/Mac1$^-$/Gr1$^-$/TCRαβ$^+$/CD4$^+$/CD8$^-$;

CD8 T cells: B220$^-$/CD19$^-$/Mac1$^-$/Gr1$^-$/TCRαβ$^+$/CD4$^-$/CD8$^+$;

HSCs: lineage (CD3, CD4, CD8, B220, Gr1, Mac1, Ter119)$^-$/IL7Rα$^-$/ckit$^+$/Sca1$^+$/Flk2$^-$/CD34$^-$/CD150$^+$;

MPP^{Flk2-} (Flk2− multipotent progenitor): lineage (CD3, CD4, CD8, B220, Gr1, Mac1, Ter119)$^-$/IL7Rα$^-$/ckit$^+$/Sca1$^+$/Flk2$^-$/CD34$^+$;

MPP^{Flk2+} (Flk2+ multipotent progenitor): lineage (CD3, CD4, CD8, B220, Gr1, Mac1, Ter119)$^-$/IL7Rα$^-$/ckit$^+$/Sca1$^+$/Flk2$^+$;

CLPs: lineage (CD3, CD4, CD8, B220, Gr1, Mac1, Ter119)$^-$/IL7Rα$^+$/Flk2$^+$;

GMPs: lineage (CD3, CD4, CD8, B220, Gr1, Mac1, Ter119)$^-$/IL7Rα$^-$/ckit$^+$/Sca1$^-$/CD34$^+$/FcγR$^+$.

ACKNOWLEDGMENTS. We thank N. Neff, G. Mantalas, T. Snyder, B. Passarelli, and S. Quake for carrying out the high-throughput sequencing; M. Inlay, T. Serwold, and C. Chan for helpful discussions on experiments; H. Nakauchi, S. Karten, K. Loh, and C. Lytal for helpful suggestions on the manuscript; L. Jerabek and T. Storm for laboratory management; C. Muscat and T. Naik for antibody conjugation; A. Mosley for animal supervision; and P. Lovelace for FACS core management and technical support. This work was supported by NIH Grants R01-CA86065 and U01-HL099999. R.L. was supported by NIH Grants K99/R00-HL113104, R01HL135292, R01HL138225, and P30CA014089. A.C. was supported by a Howard Hughes Medical Institute Medical Research Training Fellowship, a Stanford University Medical Scholars Fellowship, and The Paul & Daisy Soros Fellowship for New Americans.

1. Bryder D, Rossi DJ, Weissman IL (2006) Hematopoietic stem cells: The paradigmatic tissue-specific stem cell. *Am J Pathol* 169:338–346.
2. Seita J, Weissman IL (2010) Hematopoietic stem cell: Self-renewal versus differentiation. *Wiley Interdiscip Rev Syst Biol Med* 2:640–653.
3. Weissman IL (2000) Stem cells: Units of development, units of regeneration, and units in evolution. *Cell* 100:157–168.
4. Kondo M, et al. (2000) Cell-fate conversion of lymphoid-committed progenitors by instructive actions of cytokines. *Nature* 407:383–386.
5. Rankin EB, et al. (2012) The HIF signaling pathway in osteoblasts directly modulates erythropoiesis through the production of EPO. *Cell* 149:63–74.
6. Rieger MA, Hoppe PS, Smejkal BM, Eitelhuber AC, Schroeder T (2009) Hematopoietic cytokines can instruct lineage choice. *Science* 325:217–218.
7. Sarrazin S, et al. (2009) MafB restricts M-CSF-dependent myeloid commitment divisions of hematopoietic stem cells. *Cell* 138:300–313.
8. Beerman I, et al. (2010) Functionally distinct hematopoietic stem cells modulate hematopoietic lineage potential during aging by a mechanism of clonal expansion. *Proc Natl Acad Sci USA* 107:5465–5470.
9. Copley MR, Beer PA, Eaves CJ (2012) Hematopoietic stem cell heterogeneity takes center stage. *Cell Stem Cell* 10:690–697.
10. Dykstra B, et al. (2007) Long-term propagation of distinct hematopoietic differentiation programs in vivo. *Cell Stem Cell* 1:218–229.
11. McKenzie JL, Gan OI, Doedens M, Wang JCY, Dick JE (2006) Individual stem cells with highly variable proliferation and self-renewal properties comprise the human hematopoietic stem cell compartment. *Nat Immunol* 7:1225–1233.
12. Morita Y, Ema H, Nakauchi H (2010) Heterogeneity and hierarchy within the most primitive hematopoietic stem cell compartment. *J Exp Med* 207:1173–1182.
13. Muller-Sieburg CE, Cho RH, Karlsson L, Huang JF, Sieburg HB (2004) Myeloid-biased hematopoietic stem cells have extensive self-renewal capacity but generate diminished lymphoid progeny with impaired IL-7 responsiveness. *Blood* 103:4111–4118.
14. Sieburg HB, et al. (2006) The hematopoietic stem compartment consists of a limited number of discrete stem cell subsets. *Blood* 107:2311–2316.
15. Weksberg DC, Chambers SM, Boles NC, Goodell MA (2008) CD150- side population cells represent a functionally distinct population of long-term hematopoietic stem cells. *Blood* 111:2444–2451.
16. Sun J, et al. (2014) Clonal dynamics of native haematopoiesis. *Nature* 514:322–327.
17. Rodriguez-Fraticelli AE, et al. (2018) Clonal analysis of lineage fate in native haematopoiesis. *Nature* 553:212–216.
18. Yamamoto R, et al. (2013) Clonal analysis unveils self-renewing lineage-restricted progenitors generated directly from hematopoietic stem cells. *Cell* 154:1112–1126.
19. Cho RH, Sieburg HB, Muller-Sieburg CE (2008) A new mechanism for the aging of hematopoietic stem cells: Aging changes the clonal composition of the stem cell compartment but not individual stem cells. *Blood* 111:5553–5561.
20. Dykstra B, Olthof S, Schreuder J, Ritsema M, de Haan G (2011) Clonal analysis reveals multiple functional defects of aged murine hematopoietic stem cells. *J Exp Med* 208: 2691–2703.
21. Muller-Sieburg CE, Sieburg HB, Bernitz JM, Cattarossi G (2012) Stem cell heterogeneity: Implications for aging and regenerative medicine. *Blood* 119:3900–3907.
22. Rossi DJ, Jamieson CHM, Weissman IL (2008) Stems cells and the pathways to aging and cancer. *Cell* 132:681–696.
23. Purton LE, Scadden DT (2007) Limiting factors in murine hematopoietic stem cell assays. *Cell Stem Cell* 1:263–270.
24. Domen J, Gandy KL, Weissman IL (1998) Systemic overexpression of BCL-2 in the hematopoietic system protects transgenic mice from the consequences of lethal irradiation. *Blood* 91:2272–2282.
25. Czechowicz A, et al. (2016) Completely non-myeloablative/non-lymphoablative conditioning for BMT/HSCT using anti-ckit immunotoxins. *Blood* 128:493.
26. Czechowicz A, Kraft D, Weissman IL, Bhattacharya D (2007) Efficient transplantation via antibody-based clearance of hematopoietic stem cell niches. *Science* 318: 1296–1299.
27. Chandrakasan S, et al. (2017) KIT blockade is sufficient to sustain donor hematopoietic stem cell engraftment in fanconi anemia mice. *Blood* 129:1048–1052.
28. Dominici M, et al. (2009) Restoration and reversible expansion of the osteoblastic hematopoietic stem cell niche after marrow radioablation. *Blood* 114:2333–2343.
29. Pietras EM, et al. (2015) Functionally distinct subsets of lineage-biased multipotent progenitors control blood production in normal and regenerative conditions. *Cell Stem Cell* 17:35–46.
30. Allsopp RC, Cheshier S, Weissman IL (2001) Telomere shortening accompanies increased cell cycle activity during serial transplantation of hematopoietic stem cells. *J Exp Med* 193:917–924.
31. Ito M, et al. (2005) Stem cells in the hair follicle bulge contribute to wound repair but not to homeostasis of the epidermis. *Nat Med* 11:1351–1354.
32. Tian H, et al. (2011) A reserve stem cell population in small intestine renders Lgr5-positive cells dispensable. *Nature* 478:255–259.
33. Bhattacharya D, et al. (2009) Niche recycling through division-independent egress of hematopoietic stem cells. *J Exp Med* 206:2837–2850.
34. Goodman JW, Hodgson GS (1962) Evidence for stem cells in the peripheral blood of mice. *Blood* 19:702–714.
35. McCredie KB, Hersh EM, Freireich EJ (1971) Cells capable of colony formation in the peripheral blood of man. *Science* 171:293–294.
36. Wright DE, Wagers AJ, Gulati AP, Johnson FL, Weissman IL (2001) Physiological migration of hematopoietic stem and progenitor cells. *Science* 294:1933–1936.
37. Lu R, Neff NF, Quake SR, Weissman IL (2011) Tracking single hematopoietic stem cells in vivo using high-throughput sequencing in conjunction with viral genetic barcoding. *Nat Biotechnol* 29:928–933.
38. Brewer C, Chu E, Chin M, Lu R (2016) Transplantation dose alters the differentiation program of hematopoietic stem cells. *Cell Rep* 15:1848–1857.
39. Nguyen L, et al. (2018) Functional compensation between hematopoietic stem cell clones *in vivo*. *EMBO Rep* 19:e45702.
40. Jordan CT, Lemischka IR (1990) Clonal and systemic analysis of long-term hematopoiesis in the mouse. *Genes Dev* 4:220–232.
41. Lemischka IR, Raulet DH, Mulligan RC (1986) Developmental potential and dynamic behavior of hematopoietic stem cells. *Cell* 45:917–927.
42. Carrelha J, et al. (2018) Hierarchically related lineage-restricted fates of multipotent haematopoietic stem cells. *Nature* 554:106–111.
43. Yang L, et al. (2005) Identification of Lin(-)Sca1(+)kit(+)CD34(+)Flt3- short-term hematopoietic stem cells capable of rapidly reconstituting and rescuing myeloablated transplant recipients. *Blood* 105:2717–2723.
44. Fialkow PJ, Jacobson RJ, Papayannopoulou T (1977) Chronic myelocytic leukemia: Clonal origin in a stem cell common to the granulocyte, erythrocyte, platelet and monocyte/macrophage. *Am J Med* 63:125–130.
45. Serwold T, Ehrlich LIR, Weissman IL (2009) Reductive isolation from bone marrow and blood implicates common lymphoid progenitors as the major source of thymopoiesis. *Blood* 113:807–815.
46. Beachy PA, Karhadkar SS, Berman DM (2004) Tissue repair and stem cell renewal in carcinogenesis. *Nature* 432:324–331.
47. Cartier N, et al. (2009) Hematopoietic stem cell gene therapy with a lentiviral vector in X-linked adrenoleukodystrophy. *Science* 326:818–823.
48. Cavazzana-Calvo M, et al. (2010) Transfusion independence and HMGA2 activation after gene therapy of human β-thalassaemia. *Nature* 467:318–322.
49. Cabezas-Wallscheid N, et al. (2014) Identification of regulatory networks in HSCs and their immediate progeny via integrated proteome, transcriptome, and DNA methylome analysis. *Cell Stem Cell* 15:507–522.
50. Gerrits A, et al. (2010) Cellular barcoding tool for clonal analysis in the hematopoietic system. *Blood* 115:2610–2618.
51. Rio P, et al. (2018) Engraftment and phenotypic correction of hematopoietic stem cells in non-conditioned Fanconi anemia patients treated with ex vivo gene therapy. Available at https://plan.core-apps.com/asgct2018/abstract/b46a0669-c7f5-4444-b3e9-4a48e8da439a. Accessed August 15, 2018.
52. Wilson A, et al. (2008) Hematopoietic stem cells reversibly switch from dormancy to self-renewal during homeostasis and repair. *Cell* 135:1118–1129.
53. Prchal JT, et al. (1996) Clonal stability of blood cell lineages indicated by X-chromosomal transcriptional polymorphism. *J Exp Med* 183:561–567.
54. Orkin SH (2000) Diversification of haematopoietic stem cells to specific lineages. *Nat Rev Genet* 1:57–64.
55. Hsieh MM, et al. (2009) Allogeneic hematopoietic stem-cell transplantation for sickle cell disease. *N Engl J Med* 361:2309–2317.
56. Maloney DG, Sandmaier BM, Mackinnon S, Shizuru JA (2002) Non-myeloablative transplantation. *Hematology Am Soc Hematol Educ Program* 2002:392–421.
57. Kent DG, et al. (2009) Prospective isolation and molecular characterization of hematopoietic stem cells with durable self-renewal potential. *Blood* 113:6342–6350.